



Aggregation of soil and climate input data can underestimate simulated biomass loss and nitrate leaching under climate change

A. Villa^{a,*}, H. Eckersten^b, T. Gaiser^c, H.E. Ahrends^d, E. Lewan^a

^a Department of Soil and Environment, Swedish University of Agricultural Sciences, Uppsala, Sweden

^b Department of Crop Production Ecology, Swedish University of Agricultural Sciences, Uppsala, Sweden

^c Crop Science Group, INRES, University of Bonn, Bonn, Germany

^d Department of Agricultural Sciences, University of Helsinki, Helsinki, Finland

ARTICLE INFO

Keywords:

Winter wheat
Soil-crop model
Environmental impact
Severe biomass loss
Spatial aggregation effects
N-leaching

ABSTRACT

Predicting areas of severe biomass loss and increased N leaching risk under climate change is critical for applying appropriate adaptation measures to support more sustainable agricultural systems. The frequency of annual severe biomass loss for winter wheat and its coincidence with an increase in N leaching in a temperate region in Germany was estimated including the error from using soil and climate input data at coarser spatial scales, using the soil-crop model CoupModel. We ran the model for a reference period (1980–2010) and used climate data predicted by four climate model(s) for the Representative Concentration Pathways (RCP) 2.6, 4.5 and 8.5. The annual median biomass estimations showed that for the period 2070–2100, under the RCP8.5 scenario, the entire region would suffer from severe biomass loss almost every year. Annual incidence of severe biomass loss and increased N leaching was predicted to increase from RCP4.5 to the 8.5 scenario. During 2070–2100 for RCP8.5, in more than half of the years an area of 95% of the region was projected to suffer from both severe biomass loss and increased N leaching. The SPEI3 predicted a range of 32 (P3 RCP4.5) to 55% (P3 RCP8.5) of the severe biomass loss episodes simulated in the climate change scenarios. The simulations predicted more severe biomass losses than by the SPEI index which indicates that soil water deficits are important in determining crop losses in future climate scenarios. There was a risk of overestimating the area where “no severe biomass loss + increased N leaching” occurred when using coarser aggregated input data. In contrast, underestimation of situations where “severe biomass loss + increased N leaching” occurred when using coarser aggregated input data. Larger annual differences in biomass estimations compared to the finest resolution of input data occurred when aggregating climate input data rather than soil data. The differences were even larger when aggregating both soil and climate input data. In half of the region, biomass could be erroneously estimated in a single year by more than 40% if using soil and climate coarser input data. The results suggest that a higher spatial resolution of especially climate input data would be needed to predict reliably annual estimates of severe biomass loss and N leaching under climate change scenarios.

1. Introduction

Current agricultural production systems in many parts of the world are degrading land and water resources, biodiversity and climate (Foley et al., 2011). There is therefore a need to secure food for a growing population and, at the same time, to reduce the impact of the food production systems on the environment (Godfray et al., 2010). Climate change may aggravate these problems, with projected increases in the frequency of severe droughts, heatwaves and extreme precipitation events likely to affect crop production. Many previous studies have

focused on how future climate change may affect crop production (e.g. Challinor et al., 2010; Frieler et al., 2017; Webber et al., 2018) but fewer studies have investigated the effects on both crop production and the environment (e.g. Congreves et al., 2016; Blanke et al., 2017; He et al., 2018).

Nitrogen leaching to ground- and surface water results in several negative impacts on the environment, mainly in the form of eutrophication, acidification and toxicity of drinking water (Jones et al., 2014). Changes in the pattern and intensity of precipitation as well as changes in temperature due to climate change are expected to affect N leaching.

* Corresponding author.

E-mail address: ana.villa@slu.se (A. Villa).

<https://doi.org/10.1016/j.eja.2022.126630>

Received 31 May 2021; Received in revised form 13 June 2022; Accepted 2 September 2022

Available online 18 September 2022

1161-0301/© 2022 The Author(s). Published by Elsevier B.V. This is an open access article under the CC BY license (<http://creativecommons.org/licenses/by/4.0/>).

In many cases predictions have shown an increase of N leaching (e.g. Berit et al., 2005; Stuart et al., 2011) and different mechanisms may be responsible for this increase. Summer drought will probably increase the accumulation of N in soils (due to decreased run off and plant N uptake), which can later be mobilized by intense heavy autumn or spring rains (Loecke et al., 2017). Another likely mechanism for increased N leaching is that an increase in the frequency of large rainfall events during spring and summer, can delay sowing, plant emergence and establishment causing larger water fluxes through soil (Bowles et al., 2018).

Impacts of climate change will differ across regions. In northern Europe, the change in climate may have both positive and negative impacts. It may increase crop productivity by extending the length of the growing season and increasing the areas suitable for crop cultivation (SOU, 2007; Fogelfors et al., 2009). However, it is also expected that N leaching will increase (Olesen and Bindi, 2002). In contrast, in southern Europe, the effects of climate change will be mostly negative. An increase in extreme weather events and water shortage may result in lower yields, higher yield variability and a decrease in the area suitable for traditional crops (Hristov et al., 2020).

To identify and apply cost-effective mitigation measures it is necessary identify most vulnerable areas properly. Spatial modelling is a useful approach to identify the areas more vulnerable for losses in crop production and increased N leaching potential for present conditions and future climate scenarios. Crop models have been widely used in agricultural research, for example in developing more resilient crop varieties or analysing how management practices affect yields (e.g. Dettori et al., 2011; Wang et al., 2012). These crop models were originally developed and tested for individual fields represented by spatially homogeneous input data. Recent applications of crop models are linked to the need to explore and analyse agricultural production and environmental effects at a regional or global scale to face the challenges of climate change (e.g. Rosenzweig et al., 2014; Martre et al., 2015). Issues such as the mitigation of N and P loads to waterbodies, and future food security under climate change are a concern for decision- and policy-makers at watershed, regional, national and global scales (Hansen and Jones, 2000). The problem is that detailed soil, weather and management data needed for large-scale crop model applications are usually lacking. Spatial and temporal resolution of data on soil, climate and land management often differ and need to be disaggregated or aggregated by different methods to the desired resolution of the study concerned (Ewert et al., 2011). Such changes and differences in spatial scales might affect simulation results. In different studies for a temperate and a Mediterranean region (e.g. Hoffmann et al., 2016a; Grosz et al., 2017; Constantin et al., 2019; Maharjan et al., 2019), the error in regional yields obtained from aggregating soil and climate input data increased with decreasing spatial resolution. These studies found hot spots with very large yield differences, both positive and negative (-2 to 2 t ha⁻¹ for winter wheat in North Rhine Westphalia, Germany), where the aggregation of soil data was the main driver of the induced aggregation errors (Maharjan et al., 2019). All these studies have focused on the errors in regional model output variables (e.g. yield, drainage, soil organic carbon) for 30-year averages of a reference period (describing recent climate conditions), whereas, to the best of our knowledge, no studies could be found that focused on the effects of soil and climate data aggregation under climate change scenarios.

Adaptation to climate change (e.g. whether or not to invest in a new irrigation system) requires knowledge of both long-term changes (long term changes in precipitation patterns, invest or not in a specific irrigation system) and short-term changes (precipitation variability and extremes) due to climate change (Neil Adger et al., 2005). Moreover, it is relevant to identify the regional crop production risk under climate change, to provide a basis for estimating food security during these episodes (Webber et al., 2020). It might become more common that poor production in one area/region needs to be compensated by higher yields elsewhere at the national, EU or global scale. In this case, it is necessary to properly identify the areas where crop failure might occur and

especially when synchronous crop failures will occur (Anderson et al., 2019). In the same way, identifying areas vulnerable to N leaching would be important to select and apply best management practices. As an example, more variable weather conditions in the future are expected to reduce the effectiveness of conservation practices to control N losses. However, Congreves et al. (2016) found a greater sensitivity of N loss to future weather extremes under conventional systems than under best management systems.

Drought is expected to increase in frequency and intensity in many regions of the world due to climate change (Trnka et al., 2019), which in turn will negatively affect the production of wheat causing more often and spatially spread crop failures. Predicting drought events is therefore important to be able to forecast crop losses. A useful and widely used index to predict drought based on meteorological variables is the SPEI index (Vicente-Serrano et al., 2010). The effect though of a meteorological drought on crop growth will also be dependent on the water storage capacity of soils, which may buffer or not the impacts of drought and on the coincidence of the drought event with sensitive phenological periods of the crop (Tijdeman and Menzel, 2020). Exploring the use of SPEI can give a first glance on how important soils in the region might be in a changing climate.

The overall aim of this study is to investigate how climate change might affect severe biomass loss and N leaching in a temperate climatic region. The specific aims are to (i) estimate the change in frequency of annual severe biomass loss and its coincidence with an increase in N leaching using a crop model (ii) evaluate the use of a meteorological drought index to estimate severe biomass loss as compared to simulations with a process-based crop model, and (iii) study the role of soil and climate input data resolution in climate change impact assessments of severe biomass loss and N leaching.

2. Material and methods

2.1. Study region

The study region was the federal state of North-Rhine Westphalia (NRW, 6.0–9.5°E, 50.0–52.5°N), in west-central Germany, which has an area of 34 098 km². Half of the region is located in the flat plains of the Westphalian Lowland and Rhineland, which extend broadly into the North German Plain. The topography rises from the northwest towards the southeast with elevations ranging up to 842 m above sea level (Fig. 1). Predominant soil types are Cambisols, Luvisols and Stagnosols (FAO key reference soil groups: CM, LV, ST, respectively; FAO, 2015). NRW has a humid, temperate climate with an annual mean temperature in the period 1980–2010 of 8.1 °C and a mean annual precipitation of 591 mm. About 60% of the area is used by agriculture, with winter wheat and silage maize being the main crops. In this study, we assumed the entire region to be agricultural land cultivated with winter wheat, following an approach used in previous studies (Hoffmann et al., 2015; Zhao et al., 2015; Constantin et al., 2019). Further background information on the region can be found in different studies. Zhao et al. (2016) present a summary of climate and soil information in the form of maps of daily mean temperature, annual precipitation, global solar radiation as well as soil properties such as soil water holding capacity down to -1.5 m depth and area-dominant soil types at a spatial resolution of 1 km.

2.2. Model input data

2.2.1. Climate data

Climate data for the baseline period of 1980–2010 (P0) was taken from the Joint Research Centre's (JRC) Agri4Cast gridded dataset. It included daily records of minimum, average and maximum air temperature, precipitation, wind speed, global radiation, and actual air vapour pressure measured at standard meteorology stations and aggregated to a 25 km x 25 km grid resolution.

The reference climate time series differed from that applied in

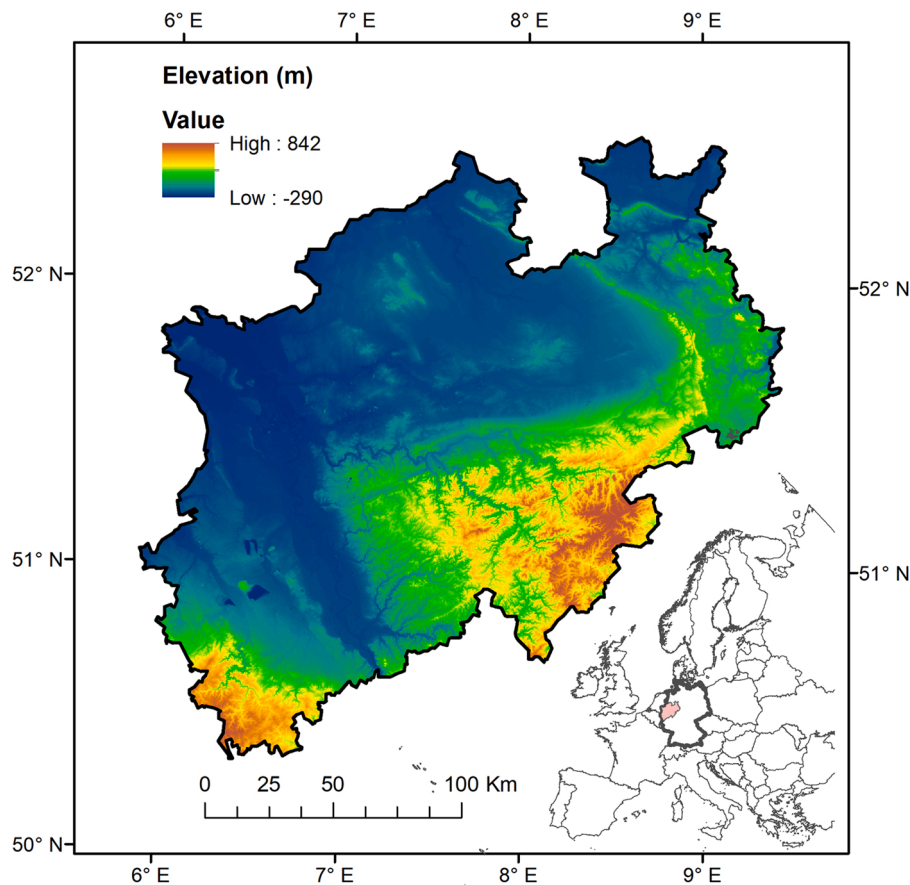


Fig. 1. Location and elevation of the state of North Rhine Westphalia (NRW), Germany. The region is coloured in pink in the smaller map of Europe (right bottom corner). Digital terrain model with 200 m grid cell obtained from the Federal Agency for Cartography and Geodesy, Germany (<http://www.bkg.bund.de>).

previous NRW-studies (Hoffmann et al., 2015, 2016a; Grosz et al., 2017; Constantin et al., 2019), due to different approaches for spatial interpolation between meteorological stations, the use of different stations and also a different geographical mesh for the grid-resolution at 25 km. Therefore, the gridded 25 km reference rainfall for NRW was lower in this study compared to the time-series applied in the previous studies. The difference in mean annual precipitation for a 25 km² grid cell ranged from 16 mm yr⁻¹ to 174 mm yr⁻¹ annually in the period 1982–2010 (annual mean difference was 93 mm yr⁻¹), resulting in lower rainfall of 2709 mm for the whole period over all grid cells. However, the crop parameterisation of the CoupModel, which was calibrated to observed average regional grain yield in these previous studies, was not changed in order to simulate the same crop and to be comparable with the ensemble of soil-vegetation models applied in the series of former studies of the NRW-region (Hoffmann et al., 2015; Hoffmann et al., 2016).

The future climate projections cover two periods, 2040–2069 (period 2, P2) and 2070–2099 (period 3, P3) as generated by five GCM models (GFDL-CM3, GISS-E2-R, HadGEM2-Es, MIROC5, and MPI-ESM-MR) under two forcing scenarios (RCP 4.5 and RCP 8.5). For RCP 2.6, projections from only two GCMs (HadGEM2-ES and MPI-ESM-MR) were available for the study. The climate projections were available at a 0.5° resolution and downscaled to the 25 km grid resolution corresponding to that of the baseline data. The climate projections were created using an enhanced delta change method (Ruane et al., 2015) where correction factors are added (air temperature) or multiplied (precipitation) to the baseline daily weather data series. The climate data is further described by Webber et al. (2015) and can be accessed at http://open-research-data-zalf.ext.zalf.de/ResearchData/DK_59.html. The impact of increased CO₂ concentrations on crop growth was not

accounted for in our study.

The annual mean temperatures are projected to increase in a range of 0.9–3.7° in the period 2040–2070 (P2) and from 0.9° to 5.6° in the period 2070–2100 (P3), depending on the RCP-GCM scenario. Concerning precipitation, there are no differences in the projected mean annual values compared to the baseline period for the grouped RCP 4.5 and 8.5 in P2. In the RCP 2.6 P2, mean annual precipitation is projected to decrease by 2%. In P3, the differences are also small, being the largest in the RCP 4.5 scenarios with an increase of 2% in mean annual precipitation. Seasonal variations in the projected changes are presented in Fig. 2 for all 24 scenarios. With scenarios representing the results from 12 different RCP-GCM combinations for periods P2 and P3. Projections of monthly precipitation in NRW vary widely between the RCP-GCM scenarios, especially in P3. Although not being consistent, there is a tendency for projected monthly precipitation to increase during the winter and decrease during the summer in most scenarios. Projected monthly temperatures show an increase for all climate scenarios and periods.

2.2.2. Soil data

Soil data for NRW (texture, soil layer thickness, gravel content) were obtained in a first step at a 300 m resolution by aggregating mapping units by areal majority using a soil map (scale 1:50,000) from the Geological Service North-Rhine Westphalia (Geological Service NRW, 2004). Soil data was then aggregated to 1 km resolution by selecting the predominant soil type present in the 300 m resolution map (Hoffmann et al., 2016a). Other soil parameters (e.g. water holding capacity, topsoil organic carbon, pH, top soil CN-ratio) were obtained as explained in Hoffmann et al. (2016a). The complete set of soil properties can be found in Hoffmann et al. (2016b) and the list of soils used specifically in

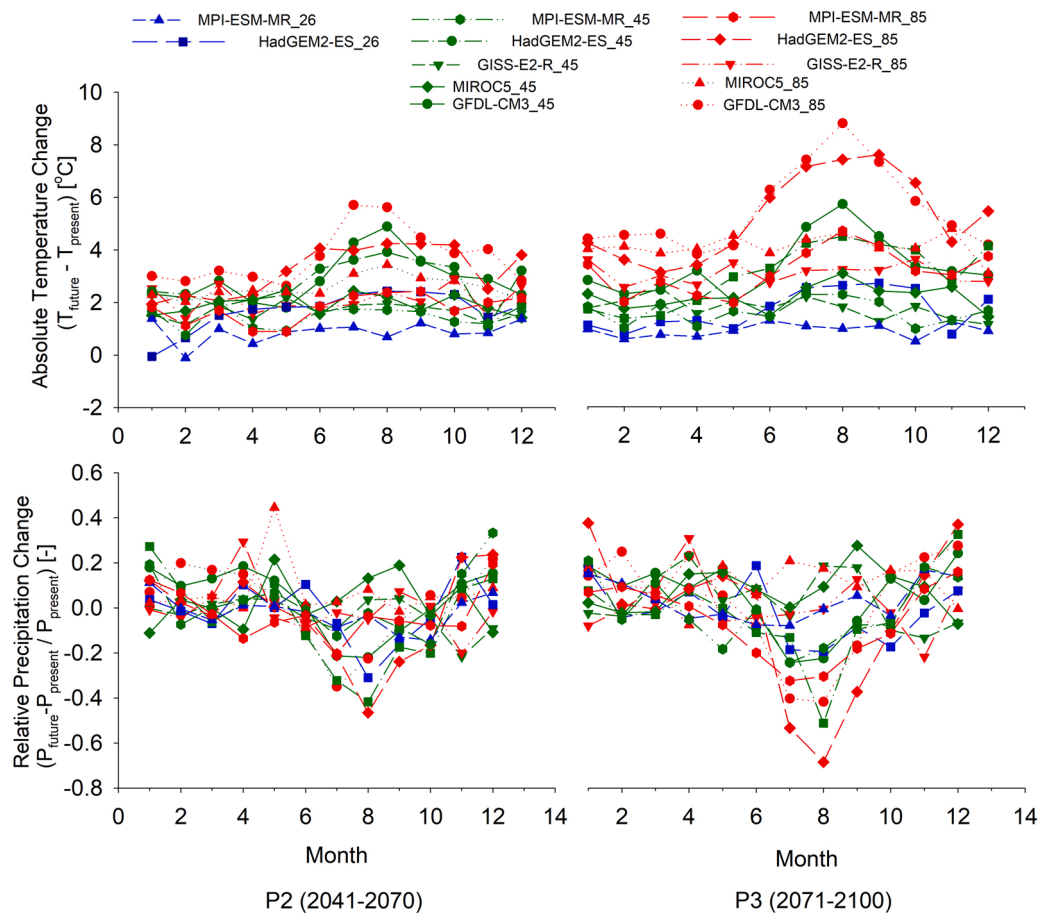


Fig. 2. Projected monthly change for temperature (left) and precipitation (right) derived from 12 different climate scenarios for NRW. The change was calculated for the future periods 2 (P2: 2041–2070) and 3 (P3: 2071–2100) compared to the reference period (1981–2010) and presented as absolute difference for temperature and relative change for precipitation. In blue different GCMs under RCP2.6, in green different GCMs under RCP4.5 and in red different GCMs under RCP8.5.

this exercise is included in the [Supplementary material \(Table S2\)](#). In a second step, soil data at the 25, 50 and 100 km² resolution were obtained by aggregating soil data available at a resolution of 1 km. Soils showed a wide range of texture, from clay soils (with up to 55% clay in topsoil and 75% clay in subsoil) to sandy soils (with up to 92% sand in both topsoil and subsoil). Soil organic carbon in topsoil ranged from 1.1% to 15% (average of 2.3%) and CaCO₃ ranged from 0% to 20% (average of 0.3%). For the 25 km resolution grids there are 63 dominant soils and associated parameter sets. The number decreases to 23 and 8 for the 50 km and 100 km resolutions respectively. At the coarser resolutions (50 and 100 km) some of the soils appearing at a resolution of 1 km were also present but in different proportions.

2.3. Soil-crop model and its parameterization

The soil-crop model used, CoupModel 5.0 ([Jansson, 2012](#)), is a one-dimensional process-based ecosystem model simulating heat, water, C and N transfer in the soil-plant-atmosphere system. It can be used to explore the potential changes in crop growth and N-leaching in relation to different climate, soil properties and management practices. The model is driven by daily meteorological data (i.e. solar radiation sum, precipitation sum, mean wind speed and mean air relative humidity), and simulates soil temperature, moisture content and water flow, evapotranspiration, soil C and N dynamics, and plant development, growth and N uptake.

Simulations were conducted and evaluated for a situation in which production is limited by N, water, temperature and radiation. The model was run constraining the maximum root depth to the maximum soil

depth (unrestricted root growth). Soil physical parameters (used as input to the soil-crop model) were estimated by applying pedotransfer functions developed for German soils ([Eckelmann et al., 2005](#)). Further explanations of the data sources and the methods to derive several soil properties are given in [Hoffmann et al. \(2016a\)](#). Sowing day was considered constant (10-Nov). Nitrogen fertilization application was also constant. Three applications of 130 kg ha⁻¹, 52 and 26, were applied on days 60, 105 and 152, respectively. Two crop residues were handled in the model, straw was removed and stubbles were left on the field (10% of the aboveground total biomass and the roots).

The model parameterization of crop growth for winter wheat applied in this study is presented in further detail in [Table S2](#). The model parameterization is the same as used in the multi-model scaling exercise reported by [Hoffmann et al. \(2016a\)](#). As described in detail in [Coucheney et al. \(2018\)](#) most parameters were assumed to be spatially uniform and either set to their default values ([Jansson and Karlberg, 2013](#)), taken from previous applications representing arable land in Northern Europe ([Conrad and Fohrer, 2009a, 2009b; Gustafsson et al., 2004](#)) or adjusted to fit mean observations for the region. Other parameters varied spatially depending on soil properties and based on the information in the NRW soil database ([Hoffmann et al., 2016b](#)). The calibration procedure is further explained in [Hoffmann et al. \(2016a\)](#) and was applied in previous studies ([Coucheney et al., 2018; Maharjan et al., 2019; Kuhnert et al., 2017; Constantin et al., 2019; Grosz et al., 2017](#)). In summary, the model was calibrated at 1 km resolution by using one typical sowing and harvest date to match the regional average of observed yields for the region. For further detailed information on the model parameterization, we refer to appendix 1 in [Coucheney et al.](#)

(2018), which presents a detailed description of the model options and parameters that were adjusted and the steps in which these were modified.

The effect of different aggregation levels were explored by aggregating soil and climate data to spatial resolutions of 25 (82 grid cells), 50 (27 grid cells) and 100 (9 grid cells) km, respectively (see Fig. S1 in Supplementary material for maps with the grid scheme). The aggregated data were used as model input for simulations of winter wheat growth. Combinations of input data at different aggregation levels are abbreviated as $S_y \times C_z$ (where S_y is the soil data at resolution y and C_z is the climate data at resolution z). Simulations were carried out for every grid cell for each of the combinations of aggregated soil and climate input, as presented in Table 1. A graphical outline of the design of the modelling exercise is presented in Supplementary material (Fig. S2).

2.4. Data analysis

Two output variables were used to assess the vulnerability of agricultural production to climate change and associated environmental impacts: (i) total above ground biomass ($\text{kg D.W. ha}^{-1} \text{y}^{-1}$) and (ii) annual nitrate leaching ($\text{kg N ha}^{-1} \text{y}^{-1}$) at a depth of 1.5 m, or in the case of shallower soils, at the bottom of the soil profile.

Above-ground biomass was considered as the output variable rather than yield because it is a more general indicator of production. It should also be more closely related to N-leaching, which is more directly controlled by N-uptake by the biomass and less by the yield.

2.4.1. Impact of climate change on output variables

The change in biomass, N leaching and drainage, respectively, in response to each climate scenario was estimated as the relative change compared with the baseline simulation (P0, 1980–2010)

$$\text{Relative change} = \frac{\text{Absolute change}}{X_{P0}} = \frac{X_{RCP\ GCM\ P2,3} - X_{P0}}{X_{P0}}$$

Where, $X_{RCP-GCM\ P2,3}$ is the output value in the future scenarios (P2: 2041–2070, P3: 2071–2100) and X_{P0} is the output value in the reference scenario (P0: 1981–2010).

An annual biomass reduction of more than 30% for a specific grid cell, year and scenario, as compared with the grid cell specific 30-yr biomass average in the baseline period, was considered as a severe biomass loss. This threshold is similar to that used by de Toro et al. (2015) when identifying effects of extreme weather events on crop yields in counties in Sweden. The fraction of grid cells in the region with a reduction of more than 30% in biomass was then used as a measure of severe biomass loss (describing strongly diminished or even absent biomass) for a certain scenario.

The increase or decrease of N leaching was evaluated, similar to the biomass change, as the percentage change with respect to the grid-specific 30-year average in the baseline period.

2.4.2. Estimation of drought

To evaluate water scarcity in the region, we used the Standardized

Table 1
Overview of simulations. Spatial resolutions in climate and soil input data.

Resolution Soil (km ²)	Resolution Climate (km ²)	Combination Code	Aggregation
25	25	$S_{25} \times C_{25}$	No aggregation – reference simulations
25	50	$S_{25} \times C_{50}$	Climate
25	100	$S_{25} \times C_{100}$	Climate
50	25	$S_{50} \times C_{25}$	Soil
100	25	$S_{100} \times C_{25}$	Soil
50	50	$S_{50} \times C_{50}$	Soil and climate
100	100	$S_{100} \times C_{100}$	Soil and climate

Precipitation Evaporation Index (SPEI) (Vicente-Serrano et al., 2010) that quantifies drought intensity at various time scales. The SPEI is based on the climatic water balance (D), estimated as the difference between monthly sums of precipitation (P) and potential evapotranspiration (PET).

$$D = P - PET$$

The SPEI was computed for the 3- and 6-month periods April–June and January–June, respectively, thus, describing the accumulated surface water balance prior to harvest. We classified drought severity into three classes: moderate (SPEI between -1.5 and -1), severe (between -2 and -1.5) and extreme (below -2). To calculate PET we used the Thornthwaite equation (Thornthwaite, 1948).

2.4.3. Scaling effects

To analyze the scaling effect, describing the change in the observation variables due to a change in the resolution of the model's input data, we calculated the single cell-single yearly differences between the disaggregated output from coarser resolutions and those simulated at the highest reference resolution (i.e. 25 km²):

$$\Delta_j = \frac{x'_j - x_j}{x_j} \times 100$$

Where, Δ_j is the percentage difference between an output variable (biomass production or N leaching) from a simulation using aggregated input data (x') and the same variable obtained from a simulation with input data at 25 km resolution to the variable at 25 km (x) at a grid cell (j) calculated for each year.

3. Results

3.1. Impacts of climate change on the growing season

Harvest days based on the reference resolution ($S_{25} \times C_{25}$) for the periods P2 (2041–2070) and P3 (2071–2100) for RCP2.6 were 17 and 16 days earlier, respectively, compared to the median harvest day for the baseline period (1981–2010) (Fig. 3). For RCP4.5, median harvest days were 27 (P2) and 29 (P3) days earlier than in the baseline period,

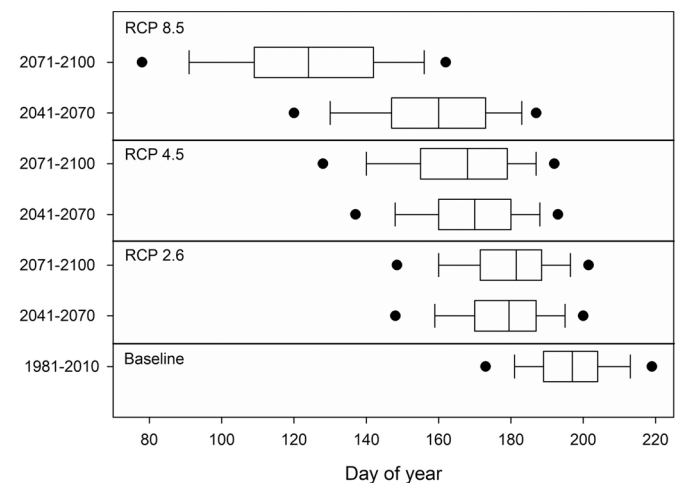


Fig. 3. Estimated harvest days for baseline and future periods under the RCP2.6, RCP4.5 and RCP8.5 scenarios. RCPs scenarios contain median days of harvest for 2 (RCP2.6) and 5 (RCP4.5 and RCP8.5) GCM. Each boxplot contain annual harvest values for all 30 years and for every grid cell in the reference resolution ($S_{25} \times C_{25}$). The solid line within the box is the median, the boundary of the box closest and farthest to zero indicates the 25th percentile and 75th percentile, respectively. Whiskers to the left and right indicate the 10th and 90th percentiles. The black dots indicate the 5th and 95th percentiles.

respectively, while for RCP8.5, the corresponding values were 37 (P2) and 73 (P3) days. The interannual variation in the day of harvest was largest for RCP8.5 and smallest for RCP2.6. Harvest days were similar between P2 and P3 for both RCP2.6 and RCP4.5, whereas for RCP8.5, the difference between P2 and P3 was substantial (36 days earlier in P3 compared to P2). The median harvest day of P3, was day number 124 (i. e. 3rd - 4th May), which was 73 days earlier than in the baseline period.

Harvest days based on simulations with aggregated input data were similar to those based on the reference (finest) resolution. The largest differences (4 days delay compared with the reference resolution) were found for RCP8.5 scenario simulations, where the climate input data had been aggregated to 100 km² grid resolution (i.e. S₂₅x C₁₀₀ and S₁₀₀x C₁₀₀; Table S3).

3.2. Simulated biomass and N leaching

The regional NRW average biomass of all grids and all years for the reference simulation resolution (25 km²) was 7.4 t DM ha⁻¹ y⁻¹ (median was 7.5 t DM ha⁻¹ y⁻¹). For the other (coarser) soil and climate resolution combinations the averages were slightly higher than for the reference (7.5–7.7 t ha⁻¹ y⁻¹), whereas minimum values were considerably higher in most cases and maximum values lower (Table 2). N leaching was more affected by the spatial aggregation of input data than biomass (except for S₂₅x C₁₀₀). As an example, at a coarser soil resolution (S₅₀x C₂₅) the maximum total annual N leaching ranged from 150.1 kg N ha⁻¹ y⁻¹ in the coarsest resolution (S₁₀₀x C₁₀₀) to 191.3 kg N ha⁻¹ y⁻¹ in the reference (S₂₅x C₂₅; Table 2).

Probability distributions of present and future biomass values as obtained when using input data at the different spatial resolutions show that simulated biomass was highest in the baseline period (Fig. S4a) and decreased in the future climate scenarios. For scenario RCP2.6, the biomass was similar for P2 and P3, whereas larger differences were found between P2 and P3 for RCP4.5 and RCP8.5. The probability of the biomass being lower than 1 t DM/ha, was close to zero (Baseline), 0.10 (P2 and P3 RCP2.6), 0.2 (P2 RCP4.5), 0.25 (P3 RCP4.5), 0.3 (P2 RCP8.5) and 0.75 (P3 RCP8.5) (Fig. S4a).

The distributions of simulated biomass were very similar for all the input data resolutions (data not shown) in the baseline period, whereas for the P3 RCP8.5 scenario the biomass was larger for the reference resolution compared to the coarser resolutions (Fig. S4b). For P3 RCP4.5, the probability of the biomass being > 6 t DM ha⁻¹ was higher for the reference resolution than for the coarser resolutions (data not shown). The opposite occurred for P3 RCP8.5 (the high-end climate change scenario), where the probability of biomass < 6 t DM ha⁻¹ was higher for the reference resolution than for the aggregated resolutions (Fig. S4b). The probability of biomass being < 1 t DM ha⁻¹ was close to 0.75, whereas for the aggregated resolutions this probability was around 0.6 (Fig. S4).

Cumulative N leaching at the end of the simulation period differed less than 11% and 5% among the aggregation levels, for the baseline period and the P3 RCP8.5 scenario (Fig. S4), respectively. Overall, the mean accumulated N leaching was larger in the reference resolution than in the coarser resolutions (Table 3). In the baseline period and in P2, larger differences (reductions) in N leaching resulted from the aggregation of soil properties than from the aggregation of climate input variables. However, these differences were small compared with the accumulated N leaching, at most 11% for the coarsest soil and climate input data (resolution S₁₀₀x C₁₀₀). In period 3, differences were larger when both soil and climate data were aggregated at 50 km². Yet, several cases of larger N leaching were also observed (in seven out of 42 cases). In these few cases N leaching in coarser resolutions were larger compared to the finest resolution. This effect was stronger (or more apparent) when aggregating only climate input data in P2 simulations, whereas in P3 simulations it was stronger when aggregating only soil data.

The average harvested aboveground biomass of the NRW region for

Table 2 Simulated average above ground biomass, annual N leaching and total water loss over the period 1980–2010 at different soil and climate resolutions over the regions of North-Rhine Westphalia. Data is presented for all 5 combinations of soil x climate input data resolutions.

	Total Above Ground Biomass (t DM ha ⁻¹)					Total annual water loss below 1.5 m (mm ha ⁻¹ y ⁻¹)					Total annual N leaching over 1.5 m (kg N ha ⁻¹ y ⁻¹)				
	Mean	Min	Max	SD	CV	Mean	Min	Max	SD	CV	Mean	Min	Max	SD	CV
S ₂₅ x C ₂₅	7.4	4.9	10.6	1.1	14.4	369.6	34.0	486.4	81.7	22.1	143.9	43.8	191.3	22.4	15.6
S ₂₅ x C ₅₀	7.6	6.4	9.2	0.6	7.8	369.1	259.2	491.8	41.9	11.4	133.2	112.6	154.1	10.5	7.9
S ₂₅ x C ₁₀₀	7.5	5.1	10.8	0.9	12.0	362.8	44.8	472.5	72.0	19.9	141.5	31.4	188.0	21.1	14.9
S ₅₀ x C ₂₅	7.5	6.0	10.0	0.8	10.4	377.1	265.6	659.3	65.1	17.3	134.7	100.0	165.2	13.7	10.2
S ₁₀₀ x C ₂₅	7.5	6.0	10.0	0.8	10.4	374.8	263.0	659.3	65.5	17.5	133.7	100.0	162.9	13.6	10.2
S ₅₀ x C ₅₀	7.5	6.4	9.2	0.6	8.0	369.5	259.1	491.7	50.5	13.7	134.1	112.6	154.1	10.4	7.7
S ₁₀₀ x C ₁₀₀	7.7	6.7	8.7	0.6	7.4	358.5	246.3	466.2	64.1	17.9	130.7	120.2	150.1	8.9	6.8

Table 3

Simulated cumulative nitrate leaching. Median cumulative nitrate leaching over NRW for each of the soil and climate combinations at the end of each of the periods, P0 (1980–2010), P2 (2040–2070), P3 (2070–2100) and under RCP 2.6, 4.5 and 8.5.

Combination	Period 0	Period 2			Period 3			
		RCP2.6	RCP4.5	RCP8.5	RCP2.6	RCP4.5	RCP8.5	
	Cumulative N leaching (at end of period) (kg N ha ⁻¹)							
S ₂₅ ×C ₂₅	4395	5558	5910	6666	5542	6223	7911	
S ₂₅ ×C ₅₀	Difference to reference resolution	-400	-136	-71	+ 8	-133	+ 51	-6
S ₂₅ ×C ₁₀₀		-156	+ 111	+ 147	-169	-212	-106	-23
S ₅₀ ×C ₂₅		-326	-430	-344	-390	-223	-54	-314
S ₁₀₀ ×C ₂₅		-363	-452	-346	-390	+ 85	+ 276	+ 250
S ₅₀ ×C ₅₀		-378	-447	-362	-437	-472	-382	-417
S ₁₀₀ ×C ₁₀₀		-482	-558	-612	-598	-129	-53	+ 67

the whole baseline period was only slightly higher when using spatially aggregated soil and climate model input data, while the interannual variation (expressed by CV) was smaller (Table 2). The effects of aggregation on an annual basis (expressed as the difference in absolute value) was larger when both climate and soil data were aggregated, being largest for the 100 km resolution aggregation. This was the case for almost all years in the baseline period (Fig. 4a) as well as in the future scenarios (RCP 2.6, 4.5 and 8.5; Fig. 4b-d). In all cases, aggregation of soil data (S₅₀×C₂₅ and S₁₀₀×C₂₅) caused a smaller median percentage difference than aggregation of climate in all cases. During the baseline period, the annual difference was less than 10% in most of the years, except for the coarsest resolution S₁₀₀×C₁₀₀ where the difference was larger than 10% in half of the years. The largest difference compared with the reference resolution was simulated in 1996, ranging from 12% (only soil S₅₀×C₂₅ and S₁₀₀×C₂₅) to 21% (both soil and climate aggregated S₁₀₀×C₁₀₀). Other years that showed large effects of aggregation on biomass production, as compared with the reference resolution, were 1990, 1997, 2006, 2007 and 2008 (Fig. 4).

For the future periods (P2 and P3, 2041–2100) with different emission scenarios, the effects of aggregating only soil inputs (i.e. S₅₀×C₂₅ and S₁₀₀×C₂₅) on biomass production were less than 10% for all years (Fig. 4b-d). The largest annual differences occurred, as in the baseline period, when aggregating both soil and climate input data. For

these resolutions the median regional difference in a single year could be up to 40% (as was the case in year 2082 for RCP4.5). This means that for half of the grid cells of the NRW region, the regional biomass was erroneously estimated by more than 40% with respect to the reference resolution. Analysis of means (ANOVA test) of the median annual biomass difference for NRW (Fig. S5) showed that in all scenarios (i.e. baseline, RCP 2.6, RCP 4.5 and RCP 8.5) the mean values from the different aggregated resolutions were significantly different (P < 0.0001). A post-hoc analysis of the means (Tukey HSD test) showed that median annual difference in biomass (%) due to aggregation of soil and climate data at 100 km (S₁₀₀×C₁₀₀) was the largest and significantly different than in all of the other resolutions in future scenarios (RCP 4.5 and RCP 8.5). In RCP 2.6, resolutions S₁₀₀×C₁₀₀ and S₅₀×C₅₀ were not significantly different. In all scenarios (present and future), the difference in biomass was significantly smaller when only soil was aggregated (S₅₀×C₂₅ and S₁₀₀×C₂₅) than aggregation of climate data alone as well as aggregation of both soil and climate data. The spread in the annual difference in the latter cases was the smallest in contrast with the largest spread, which was found when climate was aggregated to the coarsest resolution (S₂₅×C₁₀₀ and S₁₀₀×C₁₀₀).

Single cell-single year errors could be quite large, ranging from + 10.32 t DM ha⁻¹ y⁻¹ to - 13.26 t DM ha⁻¹ y⁻¹. In practice, this means that a simulated biomass of 10 t DM ha⁻¹ year⁻¹ for a reference grid cell

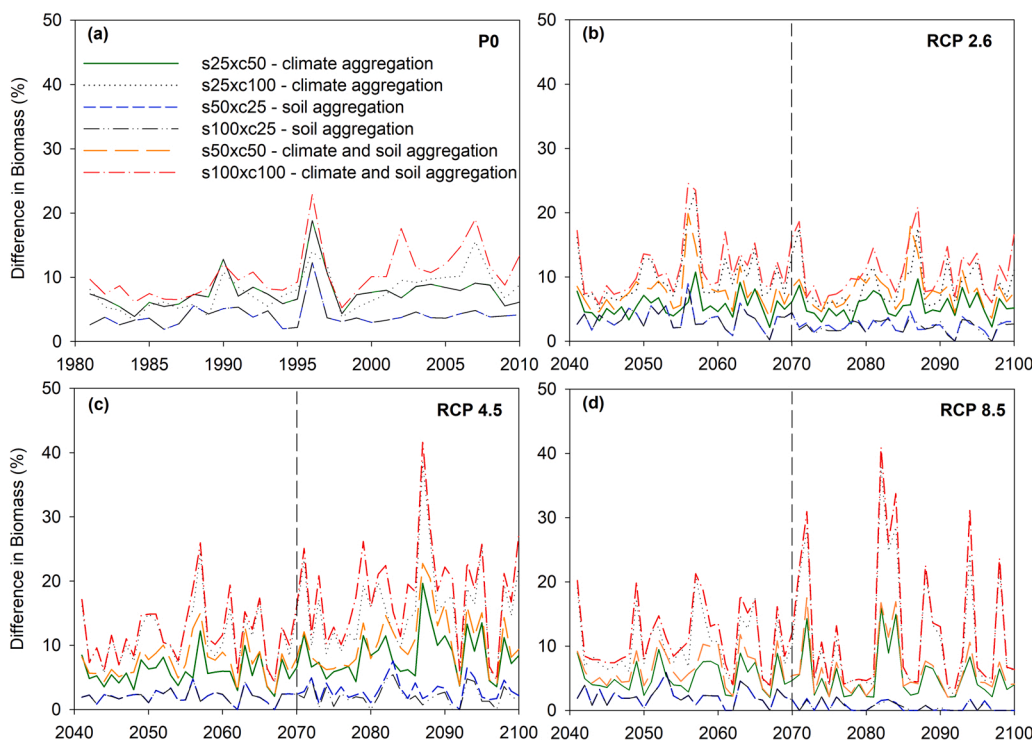


Fig. 4. Scaling effects on annual above ground biomass. Annual percentage difference (eq. 2) between aggregated resolutions and the reference resolution (s25xc25). Median values of percentage differences of all grid cells for the region NRW are shown. (a, upper left) Present conditions P0 = 1981–2010; (b-d) Future conditions P2 = 2041–2070 & P3 = 2071–2100, where in (b) (upper right) shows results based on the low emission scenario RCP2.6, (c) (lower left) moderate emission scenario RCP4.5, and, (d) (lower right) high emission scenario RCP8.5.

could be estimated as $0 \text{ t DM ha}^{-1} \text{ y}^{-1}$ at the disaggregated coarser resolution. For the resolutions with only soil aggregation ($S_{50 \times C_{25}}$ and $S_{100 \times C_{25}}$), a higher number of grid cell values deviated substantially from that of the reference grid cells. The fraction of large differences in simulated grid cell values between soil data aggregations, decreased between P2 and P3 and with a higher emission scenario being least in P3 under RCP8.5. For resolutions with aggregated climate data there were slightly more cases of overestimation but the percentage was similar to that for underestimations.

The scaling effect of aggregating both soil and climate input data is presented for mean 30 year-values for each grid cell (NRW region) (Supplementary material, Figs. S6-8) when soil and climate data are aggregated ($S_{50 \times C_{50}}$ and $S_{100 \times C_{100}}$). In all cases (except for P2 RCP 2.6), the scaling effect was larger than 24% in at least one of the grid cells of the region. Aggregation at 100 km caused larger regional 30-yr errors than aggregation at a smaller scale (50 km).

3.3. Relative changes in biomass and N leaching in response to climate change

Relative changes were analysed as annual average change over the period and all grid-cells. The above ground biomass decreased due to climate change most in RCP8.5 P3 (−83%) and least in RCP2.6 P3 (−22%) compared to the reference period. For the other scenarios the decrease was −24% (RCP2.6 P2), −35% (RCP4.5 P2), −29% (RCP4.5 P3) and −51% (RCP8.5 P2). The climate change effects in scenario RCP2.6 were on average similar for the P2 and P3, both for biomass and N leaching. In contrast to biomass production, simulated N leaching increased due to climate change. The largest and smallest responses were also for the RCP8.5 P3 (+73%) and RCP2.6 P3 (+25%) scenarios. For the other scenarios the increase was +25% (RCP2.6 P2), +37% (RCP4.5 P2), +33% (RCP4.5 P3) and +52% (RCP8.5 P2).

3.4. Severe reductions in biomass production

The mean projected proportion of grid cells in the region experiencing severe biomass loss during the future 30-year period increased from 8.3% in the baseline period to 34%, 49% and 65% by 2040–2070 for RCP2.6, RCP4.5 and RCP8.5, respectively (Fig. 5a). There were no significant changes ($\alpha = 0.01$) by 2070–2100 in the RCP2.6 and RCP4.5 scenarios compared to the period 2040–2070, whereas for RCP8.5 the area suffering severe biomass loss increased significantly to 94% by the end of the century. However, significant differences were found between P2 and P3 for RCP8.5. The annual median values suggest that from 2070, in the RCP8.5 scenario, the entire region will suffer from severely reduced biomass compared with the baseline period (Fig. 5). Significant differences among the RCPs scenarios were found in both periods and the divergence among them becomes greater during 2070–2100.

3.5. Correlation of severe biomass loss and increases in N leaching

The distribution of the annual area of NRW that suffers from different categories of risks is presented in Fig. 6. The fractional area predicted to suffer from severe biomass loss with an accompanying increase in N leaching increased in all scenarios (all future periods and emission scenarios). Severe biomass loss associated with decreased N-leaching was similar across scenarios (median ranged between 6% and 9% in all the RCPs and periods). The proportions of grid cells in the different risk categories are similar in both future time scenarios (P2 and P3) for RCP 2.6. During 2070–2100 for RCP 4.5 and 8.5, the worst-case situation (severe biomass loss + increased N leaching) will be the most common situation affecting more than half of the region. During 2070–2100 for RCP8.5, in more than half of the years an area of 95% is projected to suffer from both severe biomass loss and increased N leaching (30-year median).

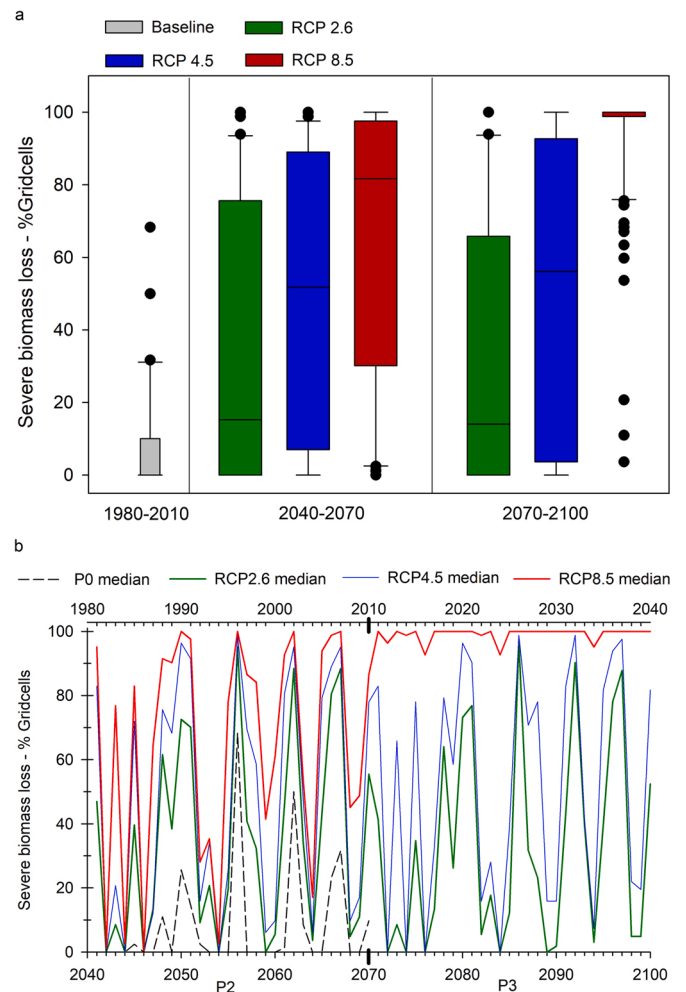


Fig. 5. Estimated proportion of grid cells for the reference resolution ($s_{25 \times c_{25}}$) showing severe biomass loss under present and future climate. (a) Distribution of the fractional area affected by severe biomass loss based on all years and grid cells. (b) Annual median values of the fractional area affected by severe biomass loss under the reference climate (P0 = 1980–2010, shown in the upper axis) and under different emission scenarios (mean of simulations with 2 GCMs for RCP2.6 and 5 GCMs for RCP4.5 and RCP8.5) for P2 (2041–2070) and P3 (2071–2100).

3.6. Implications of aggregation of input data

To assess the risk of under- or overestimating we compared the output from all resolution to the reference resolution scales at the 25 km grid cell level ($S_{25 \times C_{25}}$). The median annual fractional areas of each risk category derived from each type of input data aggregation and period are presented in Table 4. The results from the aggregated resolution were compared to the reference resolution. The differences in the estimation of “No severe biomass loss + increased N leaching” were larger than for any of the other risk categories. The annual number of grid cells that belonged to this category was consistently larger for the disaggregated results than for the reference, which means that aggregating input data overestimates the occurrence of “No severe biomass loss + increased N leaching”. The median annual difference in the fractional area affected by “no severe biomass loss and N leaching increase” was up to 45% when comparing the disaggregated coarser resolution ($S_{100 \times C_{100}}$) to the original reference resolution ($S_{25 \times C_{25}}$) (Table 4). There was a risk of overestimating situations of “no severe biomass loss + increased N leaching” when using aggregated input data. In contrast, situations of “severe biomass loss + increased N leaching” were more frequent in the original reference resolution compared to the

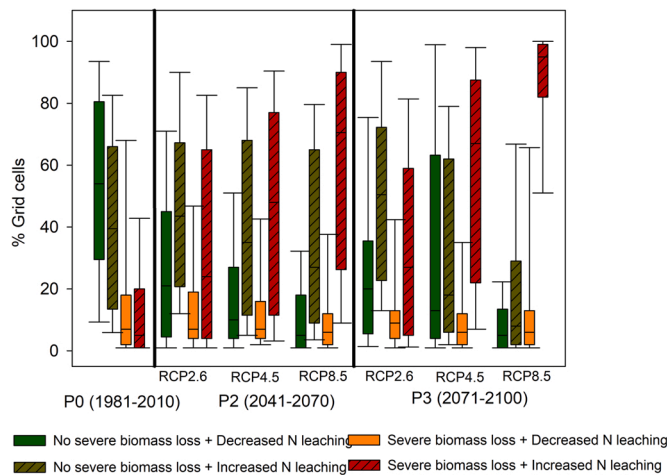


Fig. 6. Distribution of the annual fraction of grid cells in the reference resolution ($S_{25} \times C_{25}$) in the NRW region representing a combination of risk with respect to biomass loss and N-leaching, as simulated over 30 years based on 2 GCMs (RCP2.6) or 5 GCMs (RCP4.5 and RPC8.5).

disaggregated outputs from aggregated resolutions. Underestimation of the worst-case scenario (“severe biomass loss and N leaching increase”) might occur in up to 15% of the area (combination $S_{50} \times C_{25}$, P3 RCP4.5). For results derived from aggregated soil and climate data ($S_{50} \times C_{50}$ and $S_{100} \times C_{100}$) the situation was the opposite, that is, a larger fractional area was estimated from the disaggregated resolutions than from the reference resolution (Table 4).

For the other two risk categories, representing a decreased N leaching (“no biomass loss + decreased N leaching” and “biomass loss + decreased N leaching”) the difference between the annual fractional areas in the disaggregated and the reference was smaller. The difference was similar with respect to different soil and climate aggregations, but was highest for the coarsest resolution ($S_{100} \times C_{100}$). The overestimation/

underestimation was larger when N leaching increased compared to when N leaching decreased.

3.7. Use of a meteorological indicator to predict severe biomass loss and N leaching

Annual mean SPEI values for the NRW region are presented in Fig. 7. In the baseline period SPEI3 values were larger than -1.5 except for one year (1988) only. In this year, 71 % of the grid cells in the region suffered from severe drought ($SPEI < -1.5$). Values were below -1 (moderate drought) in only two other years (1996 and 2010).

In the period 2040–2070, SPEI3 values decreased compared with the baseline period (Fig. 7) indicating an increase in the number of drought events and in their severity. The fraction of the region that suffered from severe drought also increased, being up to 90% in one year (2047). A large fraction of the region is projected to suffer from severe drought ($>80\%$) in that same year, under all RCPs. During P2 the differences between RCP4.5 and RCP8.5 were small. The mean SPEI3 values fall into the same drought category for these two emission scenarios, every year. In the period 2070 – 2100 (P3), differences between RCP4.5 and RCP8.5 were larger. For RCP8.5, the number and intensity of drought events increased. In 17 years during the 30-year period, SPEI3 was below -1.0 (moderate drought) and in 10 years of the period, more than half of the region SPEI3 was below -1.5 .

3.7.1. Relation between SPEI and simulated severe biomass loss and N leaching

The simulated annual mean biomass was significantly smaller when $SPEI3 < -1.5$ compared to when $SPEI > 1.5$, for all periods and scenarios (Table S5). The annual regional mean N leaching was also significantly smaller when $SPEI3 < -1.5$ in all scenarios except for P0 and P3 RCP8.5, although mean values were similar in both groups.

The relation between simulated severe biomass loss and SPEI was explored for different SPEI values for the reference resolution $S_{25} \times C_{25}$ (Table 5). Results showed that the coincidence between SPEI and severe

Table 4

Grid cells in each of the crop failure and N leaching groups for different RCPs and periods (annual median percentage is given). The number of grid cells are the same in all of the resolutions as the results were disaggregated to the reference resolution prior to the calculations.

		P0	P2			P3		
		NA	RCP 2.6	RCP 4.5	RCP 8.5	RCP 2.6	RCP 4.5	RCP 8.5
$S_{25} \times C_{25}$	No Biomass Loss +	55	21	10	5	20	13	5
	Decreased N leaching	60	15	7	4	11	6	2
	$S_{25} \times C_{50}$	48	21	11	9	17	11	6
	$S_{50} \times C_{25}$	56	27	13	10	15	7	2
	$S_{100} \times C_{25}$	57	28	12	11	16	9	6
$S_{50} \times C_{50}$		59	30	16	12	23	16	10
	$S_{100} \times C_{100}$	66	30	29	16	21	16	10
	$S_{25} \times C_{25}$	40	44	35	27	51	18	9
	$S_{25} \times C_{50}$	46	59	49	35	60	48	18
	$S_{25} \times C_{100}$	49	59	61	63	65	60	48
$S_{50} \times C_{25}$		46	49	39	28	54	35	12
	$S_{100} \times C_{25}$	44	48	39	27	59	44	16
	$S_{50} \times C_{50}$	51	50	39	33	60	43	22
	$S_{100} \times C_{100}$	50	55	61	57	67	63	50
	$S_{25} \times C_{25}$	5	24	48	71	27	67	95
$S_{25} \times C_{50}$	Biomass Loss +	21	16	43	70	13	55	93
	Increased N leaching	9	22	45	79	49	67	94
	$S_{50} \times C_{25}$	7	23	46	67	24	52	88
	$S_{100} \times C_{25}$	7	21	45	67	18	54	88
	$S_{50} \times C_{50}$	23	57	59	79	44	68	94
$S_{100} \times C_{100}$		15	62	68	84	41	67	100
	$S_{25} \times C_{25}$	7	7	7	6	9	6	6
	$S_{25} \times C_{50}$	10	2	5	4	4	5	5
	$S_{25} \times C_{100}$	10	10	10	7	9	10	6
	$S_{50} \times C_{25}$	10	11	12	9	6	9	9
$S_{100} \times C_{25}$		11	11	13	10	9	7	10
	$S_{50} \times C_{50}$	10	15	12	10	15	10	10
	$S_{100} \times C_{100}$	13	29	29	15	18	15	15

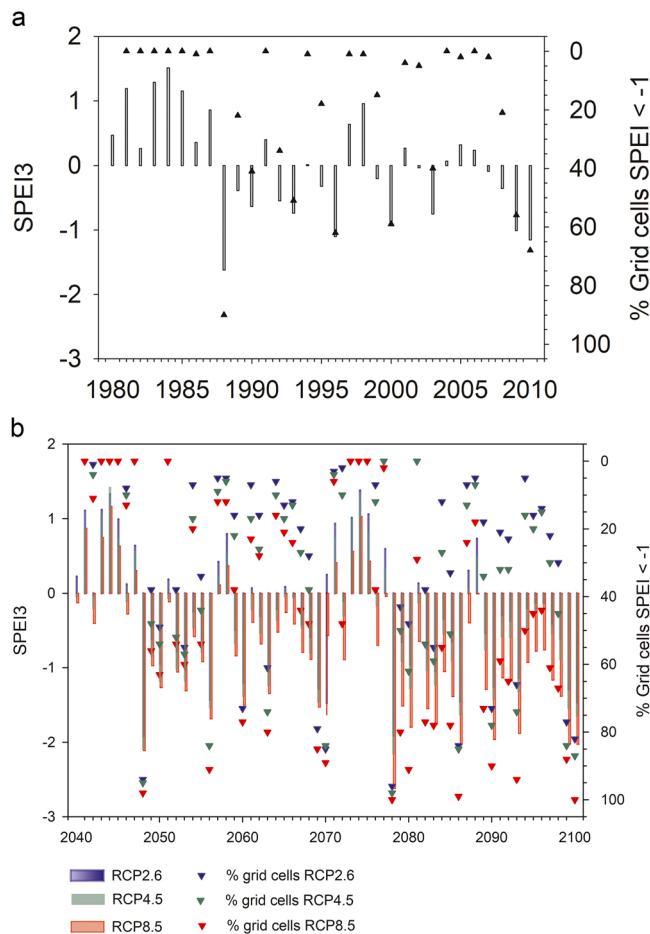


Fig. 7. Annual evolution of the drought index SPEI3 in present climate conditions, 1980–2010 (above) and in future climate scenarios, 2040–2100 (below), depending on assumed RCP scenario. Bars represent mean annual values of SPEI 3 (three months accumulated values in June every year. That is April, May and June) over North-Rhine Westphalia at a 25 × 25 km grid cell resolution. Triangles represent the % grid cells in a year in which SPEI3 < −1.

Table 5

Simulated crop failure with CoupModel for different drought intensities estimated with the SPEI index in resolution 25 × 25 km. Number of years and grid cells in NRW for which each estimation is made is calculated. Results for coincidence of crop failure and SPEI index in a given year is given in form of % over the total number of crop failure episodes. RCPs are median values of 2 (RCP2.6) and 5 (RCP4.5, RCP8.5) GCMs. SPEI is calculated for 3 months (SPEI3) of accumulated data (April, May, June) and for 6 months (SPEI6) of accumulated data (January to June).

Resolution	Period RCP	SPEI3 (< −1.5)	SPEI3 (< −1)	SPEI6 (< −1.5)	SPEI6 (< −1)
S ₂₅ ×C ₂₅	Baseline	18	46	37	47
	P2	24	40	22	41
	RCP2.6				
	P2	25	41	26	48
	RCP4.5				
	P2	20	35	22	38
	RCP8.5				
	P3	24	41	20	37
	RCP2.6				
	P3	17	32	21	38
	RCP4.5				
	P3	38	55	40	54
RCP8.5					

biomass loss events was greater with respect to moderate drought (SPEI < −1) instead of severe drought (SPEI < −1.5). The use of longer time scales to define a drought episode, i.e. 3 or 6 months of accumulated precipitation and ET data, did not have a large effect on the coincidence with severe biomass loss. The prediction of severe biomass loss episodes could be expected to be best represented by SPEI3 and most frequently associated with moderate drought (SPEI3 < −1). In this study, the SPEI3 predicted 55% of the severe biomass loss episodes simulated for the P3 RCP8.5 (Table 6). The poorest correlation between simulated severe biomass loss episodes and SPEI3-predictions was obtained for P3 with RCP4.5.

Overall, the results showed that there was a larger number of severe biomass loss episodes according to the simulations than was defined by SPEI3 (Table S6). The number of times when severe biomass loss was simulated but SPEI predicted “no drought” increased with higher RCP scenarios in all resolutions, being larger in RCP8.5 considering both P2 and P3.

4. Discussion

4.1. Crop growth stages changes

Using climate change scenarios the CoupModel predicted between two (RCP2.6) and five weeks (RCP8.5) earlier harvest dates for winter wheat compared with the baseline period. The earlier harvest dates are in accordance with other studies (Olesen et al., 2012; He et al., 2020), and in magnitude similar to projections by Semenov (2009), who predicted that maturity date would occur 21 days earlier under projected climate change in 2050 in England and Wales. A simulation study from an arid climate showed that the crop-growing season will be shortened by 10.7–21.6 days under RCP-4.5 and by 25.8–45.5 days under RCP-8.5 (Nouri et al., 2016).

The temperature sum needed for achieving maturity was set to the same value as the one used in previous studies of the NRW region, which had been adjusted to fit the observed regional harvest date of the baseline period (1980–2010) (Hoffmann et al., 2015; Coucheney et al., 2018). Thus, the scenarios assumed the winter wheat cultivar to remain unchanged in the future scenarios, as concerns its phenology response to climate. It is, however, expected that any cultivar adjustment to increased temperature would be to reduce its temperature sensitivity (Rezaei et al., 2018). Therefore, our approach might have exaggerated earlier harvest dates. The simulated harvest date response to increased temperature corresponded to a sensitivity of 12–13 days per 1 °C, for both RCP2.6 and RCP4.5, and 2040–2070 and 2070–2100. In the high emission scenario (RCP8.5) the corresponding sensitivity was a few days larger (14–17 days per 1 °C; Table S3 and Table S4). This seems to be an essentially higher sensitivity than observed in Swedish practical agriculture (1988–2010), where the date of winter wheat DC 31-development stage was estimated for regional differences to be 6 days °C⁻¹ (Eckersten and Kornher, 2012). In a European study, Olesen et al. (2012) assumed some adaptation of different crop varieties by relating the required temperature sums demands to long-term mean temperature at the specific location. They projected advances in flowering and maturity by 1–2 weeks for winter wheat depending on climate change scenario (two GCM/RCM representing the low and high end of the range of projected patterns for period 2030 –2050) and region, which is also about half the response to climate change as compared to our study. Eckersten and Kornher (2012) projected about one and a half to two and a half weeks advanced development stages under climate change.

4.2. Severe biomass loss

The crop yield simulations projected that the majority of the NRW region would suffer from severe biomass loss in some years. This was especially true for the high emission scenario of period 3 (RCP8.5), but also for the scenario RCP2.6 the incidence of severe biomass loss

Table 6

Coincidence of prediction of simulated crop failure and SPEI3 drought (<-1). % of coincidence over total crop failure episodes.

Combination (soil x climate resolution)	S ₂₅ X _{C25}	S ₂₅ X _{C50}	S ₂₅ X _{C100}	S ₅₀ X _{C25}	S ₁₀₀ X _{C25}	S ₅₀ X _{C50}	S ₁₀₀ X _{C100}
(%)							
Baseline	46	42	50	40	40	39	47
P2 RCP2.6	40	35	36	39	39	33	34
P2 RCP4.5	41	37	38	40	40	37	39
P2 RCP8.5	35	36	35	35	35	37	35
P3 RCP2.6	41	37	37	41	41	35	36
P3 RCP4.5	32	34	35	37	34	31	36
P3 RCP8.5	55	57	63	56	56	59	63

increased by up to 32% during 2041 – 2070. This is in line with a European-scale study by [Blanke et al. \(2017\)](#) who predicted an increased trend of yield uncertainty during 2031 – 2050 in the western part of NRW (recorded from maps). On the other hand, other studies have projected overall simulated yield increases in Northern Europe ([Olesen and Bindi, 2002](#)) which is in contrast to the decrease in biomass simulated in our study.

Drought has been identified as an important factor that cause severe biomass loss. Especially severe droughts have been predicted to cause widespread crop failures ([Leng and Hall, 2019](#); [Webber et al., 2020](#)). [Trnka et al. \(2019\)](#) projected that severe water scarcity events might affect several world major crop production areas simultaneously under climate change (especially towards the end of 21st century). Estimations by [Trnka et al. \(2019\)](#) were based on the precipitation-evaporation SPEI index, which predicted a stronger drought influence on crop growth during the later stages (spring and summer), rather than in the earlier stages of the plant cycle (autumn and winter). In our study, results showed that the SPEI3 index (estimated for 3 months prior to expected harvest date) was more strongly correlated with biomass than SPEI indices estimated for longer timescales. The SPEI6 index (6 months prior harvest date) predicted severe biomass loss similar to those by SPEI3 index. Similarly, [Ribeiro et al. \(2019\)](#) found that remote sensing and multi-scalar meteorological indicators displayed greatest influence on yield losses during the later stages of the plant cycle.

When comparing the simulated crop yield failures with those predicted by the SPEI index it was found that the simulations predicted severe biomass loss more often than the SPEI index, especially for RCP8.5 scenarios. One explanation might be that soil water deficit becomes more important in defining simulated severe biomass loss using dynamic simulation approaches, whereas the SPEI index (which, being based on the climatic water balance, does not explicitly consider the effects of soil water conditions effects on crop growth) did not take into soil-type specific drought responses. How different types of soils influence the crop under climate change have been studied by e.g. [Nouri et al. \(2016\)](#) who predicted more frequent harvest failure to occur on finer-textured soils, in a simulation study using CSM-CERES-Wheat v.4.6 model. In our study it was difficult to evaluate effects of different soil types, since each grid cell had both a specific soil and a specific climate, and effects of soil conditions could not be separated from those of climate. Another possible explanation of the discrepancies could be that climate-related catastrophes are a result of compound events (e.g. drought and heat) ([Zscheischler et al., 2018](#)). Thus, severe biomass losses are not being caused solely by drought but by a combination of different processes, such as the interactions between temperature and drought ([Matiu et al., 2017](#)). In a study in Germany, [Webber et al. \(2020\)](#) associated severe drought with past annual severe biomass loss whenever the failures were widespread across crops but could not identify a single driver or combination of drivers associated with annual severe biomass loss whenever these were more localized and spread in space.

Our study suggests that mitigation and adaptation measures will be needed to reduce the impacts of climate change on the agriculture and the environment in this region by increasing agricultural productivity

and thereby contributing to food security. Different approaches can be used to improve crops such as the use of new crop varieties that are better adapted to the variability of climate conditions (e.g. [van Etten et al., 2019](#)); use of more drought resistant crops ([Daryanto et al., 2017](#)), or even change of crops. Combining winter crops with cover crops is also an alternative to protect bare soils and reduce drainage and N-leaching ([Kaye and Quemada, 2017](#)). [Olesen et al. \(2011\)](#) studied a range of future adaptation strategies for European environmental zones such as cultivation timing, tillage and fertilisation practices, use of new cultivars, crop protection, seasonal weather forecasting or crop insurance. They observed that farmers across Europe are already adapting to climate change, in terms of changing the timing of cultivation and selecting different crop species and cultivars. They also found that climate change effects would still be mostly negative in most regions across Europe even when considering a wide range of adaptation options. The impact of increased CO₂ concentrations on crop growth was not accounted for in our study. However, it is unlikely to have significantly affected the simulations of the occurrence of severe biomass loss, especially considering the large uncertainties and differences among GCM-RCM future climate scenarios with respect to precipitation amounts.

4.3. N leaching

Simulated N leaching was larger in the high emission scenario (RCP8.5) as compared to RCP4.5, similar to the results of [He et al. \(2020\)](#). The increase in N leaching was probably caused by an increase in temperature, which, on average, was 4 °C higher in the RCP8.5 scenario than in the baseline scenario. This response could be explained by an increased N mineralization in response to higher temperature and thus larger amounts of mobile nitrate in the soils, but also reduced plant N uptake due to reduced growth and earlier harvest dates. Another factor contributing to increases in N leaching could be an increase in water drainage. However, increases in N leaching were weakly correlated with increases in soil water percolation in the majority of the grid cells (median values were <0.6 for all scenarios and resolutions). Also [He et al. \(2020\)](#) found no relation between increases in soil water drainage and increases of nitrate leaching even if in their study N leaching did not increase significantly from the baseline period.

Annual precipitation showed no large projected changes ([Table S4](#)), although changes in the annual pattern could contribute to N leaching increases. Projected total precipitation decreased during June-September and slightly increased during January-May and November-December ([Fig. 2](#)). The weak relative changes of precipitation might be a reason for the low correlation between changes in precipitation sums and changes in N leaching. In addition, other simulation studies have shown that in Northern Europe, simulated N leaching is affected more strongly by temperature than precipitation changes ([Børgesen and Olesen, 2011](#)). This was the case even in a Mediterranean climate in Australia, although mainly for sandy soils (where larger N leaching usually occurs), whereas heavier clay soils were more vulnerable to reduced rainfall ([Ludwig and Asseng, 2006](#)).

During the baseline period the most common cases (considering all

years and grids) in NRW were the ones characterized by “no severe biomass loss + decrease in N leaching”. In the future scenarios, however, the cases with combined negative impacts (severe biomass loss and/or increase in N-leaching) became more frequent. In RCP2.6, environmental impacts (i.e. increased N-leaching) were more frequent than crop production impacts (i.e. reduced crop yield). In the RCP4.5 and RCP8.5 scenarios, both crop production and environmental impacts became more frequent and widespread during 2040–2100. This is in contrast to the results from [Blanke et al. \(2017\)](#), who showed that N-leaching simulated with LPJ-GUESS global vegetation model was lower in RCP4.5 as compared with the high emission scenarios. Our study suggests that increases in N-leaching would be more frequent and widespread than severe biomass loss in the lower emission scenarios (RCP2.6). In RCP4.5 and RCP8.5, crop production and environmental impacts together would become more frequent and widespread during 2040–2100.

4.4. Aggregation effect

The use of coarser spatial resolution of input data in the climate change impact assessments had less influence on the predictions of regional averages than on single grid cells outputs, and a higher influence on annual outputs than period averages. Previous simulation studies of the same region during the baseline period (1980–2010) showed similar effects of scaling of climate inputs in the region and also that scaling and management effects were more obvious when analysing impacts for individual years than on the 30-year mean ([Kuhnert et al., 2017](#)). The use of coarser climate data is of particular importance when predicting the impacts of climate change on agroecosystems since the data aggregation might result in either underestimations or overestimations of impacts, as shown in our study. [Morrison et al. \(2019\)](#) also suggested that the effects of climate change may be overestimated or underestimated when using coarse climate data. The greater impact of climate input data over soil input data on yield outputs under climate change that was seen in the present study contrasts with other results from the same region where soil input data had a greater effect on simulated yields ([Hoffmann et al., 2016](#); [Maharjan et al., 2019](#)). This suggests that aggregation of climate input data is more important in climate change assessments, while aggregation of soil input data has a greater impact on simulations of yield in the present climate.

When estimating the impacts of both severe biomass loss and N leaching at the different spatial resolutions, there was a greater error in the estimations for those cases (year and/or grid cell) when N leaching was higher than the regional/period average ([Table S7](#)). The fraction of area that was incorrectly estimated was especially large for cases of “no severe biomass loss + increased N leaching”. Similarly, ([Coucheney et al., 2018](#)) showed how aggregation of climate input data had a greater effect on N-leaching than other output variables such as yield and drainage.

This study is a first approach to studying soil and climate input data aggregation error under climate change and therefore, there are several limitations that need to be explored in future studies. A number of soil-crop models should be used to understand the sources of uncertainty in the severe biomass loss and N leaching projections. For instance, the sensitivity to e.g. drought might differ between models. Different regions should also be used as the dominant source of uncertainty could be different in different locations. While in some locations the main uncertainty is GCMs in other locations is crop models ([Wang et al., 2020](#)).

The simulated soil water availability was lower than in previous studies for the region ([Hoffmann et al., 2016a](#); [Maharjan et al., 2019](#)). In addition, the sensitivity of the CoupModel to changes in water availability resulted in systematically smaller biomass for the 25 km-resolution reference climate in this study, compared to these previous studies and the observed yields for the 1 km-resolution reference climate. Theoretically, such a lower biomass has much lower N demand and hence N uptake. Consequently, the applied amount of

fertilizer in the simulations was actually too high and therefore, high amount of N was available for leaching. Therefore, the absolute N leaching rate are probably overestimated. We decided to retain the original representation of the crop to compensate for changes in weather input data that might be due to the new reference-climate data only being available at 25 km-resolution. The focus of this study is on “relative changes in biomass and N-losses” between the reference and the future climate scenarios and not on absolute values. The future climate scenarios also imply a large variation between GCMs and therefore large uncertainties in terms of future rainfall amounts and changes in temperature. This study demonstrates a method for how the vulnerability to climate change with respect to agricultural productivity and environmental impact, could be studied for a region.

5. Conclusions

Simulations with the soil-crop model CoupModel suggested that severe biomass loss will become more frequent by the end of the century (2070–2100) under the high emission scenario (without any climate change mitigation). In the worst-case scenario, the majority of the region was predicted to suffer simultaneously from severe biomass loss in many consecutive years, which might have implications for food security, for the food market and for the economy of smallholder farmers. Moreover, in all future scenarios predictions showed an increase of the area fraction across the region that will suffer from both severe biomass loss and increased N leaching. Adaptation measures to climate change would need to aim towards a maintenance of crop productivity as well as a decrease in N leaching. The results presented in this study showed how climate change might exacerbate several problems at the same time, which are of importance in the identification of mitigation and adaption strategies to support a more sustainable agriculture. The use of a meteorological index SPEI to predict severe biomass losses have highlighted the importance of considering the effects of soil properties on drought risk. More severe biomass losses were predicted by the simulations than by the SPEI index which indicates that soil water deficits are important in determining crop losses in future climate scenarios.

Aggregation of soil and climate data showed that regional biomass estimates for the reference resolution were similar to those estimated at coarser resolutions. Larger errors due to data aggregation were obtained in annual biomass and N leaching values, where aggregating climate data rather than soil data caused larger errors and underestimated the area affected by severe biomass loss and the increase of N leaching. Special attention should be paid to the resolution of climate and soil data when making annual assessments of crop production and environmental impacts in future climate scenarios. Annual assessments are important when studying the impacts of extreme events and results from this study showed that half of the grid cells in a region could have an error in predicted biomass of more than 40% with respect to the reference resolution.

CRedit authorship contribution statement

Villa A.: Conceptualization, Formal analysis, Writing – original draft, Visualization. **Eckersten H.:** Conceptualization, Writing – review & editing. **Gaiser T.:** Data curation, Conceptualization, Validation, Writing – review & editing. **Ahrends H.E.:** Writing – review & editing, Visualization. **Lewan E.:** Supervision, Conceptualization, Writing – review & editing, Project administration, Funding acquisition.

Declaration of Competing Interest

The authors declare that they have no known competing financial interests or personal relationships that could have appeared to influence the work reported in this paper.

Acknowledgements

The study was conducted within the FACCE JPI “Modelling European Agriculture with Climate Change for Food Security” (MACSUR – BB/N004922/1). It was supported by The Swedish research Council for Environment, Agricultural Sciences and Spatial Planning (220-2007-1218). All colleagues of the MACSUR scaling group are gratefully acknowledge. We are also very grateful to Professor Nicholas Jarvis (SLU, Uppsala) for constructive comments on the manuscript.

Appendix A. Supporting information

Supplementary data associated with this article can be found in the online version at doi:10.1016/j.eja.2022.126630.

References

- Anderson, W.B., Seager, R., Baethgen, W., Cane, M., You, L., 2019. Synchronous crop failures and climate-forced production variability. *Sci. Adv.* 5, 9. <https://doi.org/10.1126/sciadv.aaw1976>.
- Berit, A., Johan, A., Sofia, F., Holger, J., Charlotta, B.P., Kristian, P., 2005. Climate change impact on water quality: model results from Southern Sweden. *Ambio* 34, 559–566. (<http://www.jstor.org/stable/4315653>).
- Blanke, J.H., Olin, S., Stürck, J., Sahlin, U., Lindeskog, M., Helming, J., Lehsten, V., 2017. Assessing the impact of changes in land-use intensity and climate on simulated trade-offs between crop yield and nitrogen leaching. *Agric. Ecosyst. Environ.* 239, 385–398. <https://doi.org/10.1016/j.agee.2017.01.038>.
- Borgesen, C.D., Olesen, J.E., 2011. A probabilistic assessment of climate change impacts on yield and nitrogen leaching from winter wheat in Denmark. *Nat. Hazard. Earth Syst. Sci.* 11, 2541–2553. <https://doi.org/10.5194/nhess-11-2541-2011>.
- Bowles, T.M., Atallah, S.S., Campbell, E.E., Gaudin, A.C.M., Wieder, W.R., Grandy, A.S., 2018. Addressing agricultural nitrogen losses in a changing climate. *Nat. Sustain.* 1, 399–408. <https://doi.org/10.1038/s41893-018-0106-0>.
- Challinor, A.J., Simelton, E.S., Fraser, E.D.G., Hemming, D., Collins, M., 2010. Increased crop failure due to climate change: assessing adaptation options using models and socio-economic data for wheat in China. *Environ. Res. Lett.* 5, 034012 <https://doi.org/10.1088/1748-9326/5/3/034012>.
- Congreves, K.A., Dutta, B., Grant, B.B., Smith, W.N., Desjardins, R.L., Wagner-Riddle, C., 2016. How does climate variability influence nitrogen loss in temperate agroecosystems under contrasting management systems? *Agric. Ecosyst. Environ.* 227, 33–41. <https://doi.org/10.1016/j.agee.2016.04.025>.
- Conrad, Y., Fohrer, N., 2009a. Application of the Bayesian calibration methodology for the parameter estimation in CoupModel. *Adv. Geosci.* 21, 13–24. <https://doi.org/10.5194/adgeo-21-13-2009>.
- Conrad, Y., Fohrer, N., 2009b. Modelling of nitrogen leaching under a complex winter wheat and red clover crop rotation in a drained agricultural field. *Phys. Chem. Earth* 34, 530–540. <https://doi.org/10.1016/j.pce.2008.08.003>.
- Constantin, J., Raynal, H., Casellas, E., Hoffmann, H., Bindi, M., Doro, L., Eckersten, H., Gaiser, T., Grosz, B., Haas, E., Kersebaum, K.-C., Klatt, S., Kuhnert, M., Lewan, E., Maharjan, G.R., Moriondo, M., Nendel, C., Roggero, P.P., Specka, X., Trombi, G., Villa, A., Wang, E., Weihermüller, L., Yeluripati, J., Zhao, Z., Ewert, F., Berge, J.-E., 2019. Management and spatial resolution effects on yield and water balance at regional scale in crop models. *Agric. Meteorol.* 275, 184–195. <https://doi.org/10.1016/j.agrformet.2019.05.013>.
- Coucheney, E., Eckersten, H., Hoffmann, H., Jansson, P.E., Gaiser, T., Ewert, F., Lewan, E., 2018. Key functional soil types explain data aggregation effects on simulated yield, soil carbon, drainage and nitrogen leaching at a regional scale. *Geoderma* 318, 167–181. <https://doi.org/10.1016/j.geoderma.2017.11.025>.
- Daryanto, S., Wang, L., Jacinthe, P.-A., 2017. Global synthesis of drought effects on cereal, legume, tuber and root crops production: a review. *Agric. Water Manag.* 179, 18–33. <https://doi.org/10.1016/j.agwat.2016.04.022>.
- Dettoni, M., Cesaraccio, C., Motroni, A., Spano, D., Duce, P., 2011. Using CERES-Wheat to simulate durum wheat production and phenology in Southern Sardinia, Italy. *Field Crop. Res.* 120, 179–188. <https://doi.org/10.1016/j.fcr.2010.09.008>.
- Eckersten, H., Kornher, A., 2012. Klimatförändringars effekter på jordbrukets växtproduktion i Sverige – scenarier och beräkningssystem. (Climate change impacts on crop production in Sweden – scenarios and computational framework). Ecology. Uppsala. ISBN 978-91-576-9067-8. (https://pub.epsilon.slu.se/8590/1/eckersten_h_120208.pdf).
- Ewert, F., van Ittersum, M.K., Heckelet, T., Therond, O., Bezlepina, I., Andersen, E., 2011. Scale changes and model linking methods for integrated assessment of agricultural systems. *Agric. Ecosyst. Environ.* 142, 6–17. <https://doi.org/10.1016/j.agee.2011.05.016>.
- FAO 2015. World reference base for soil resources 2014. International soil classification system for naming soils and creating legends for soil maps. Update 2015. Food and Agricultural Organization of the United Nations. World Soil Resources Reports 106. ISSN 0532-0488.
- Fogelfors, H., Wivstad, M., Eckersten, H., Holstein, F., Johansson, S., Verwijst, T., 2009. Strategic analysis of Swedish agriculture.
- Foley, J.A., Ramankutty, N., Brauman, K.A., Cassidy, E.S., Gerber, J.S., Johnston, M., Mueller, N.D., O’Connell, C., Ray, D.K., West, P.C., Balzer, C., Bennett, E.M., Carpenter, S.R., Hill, J., Monfreda, C., Polasky, S., Rockström, J., Sheehan, J., Siebert, S., Tilman, D., Zaks, D.P.M., 2011. Solutions for a cultivated planet. *Nature* 478, 337. <https://doi.org/10.1038/nature10452>.
- Frieler, K., Schaubberger, B., Arneth, A., Balkovic, J., Chryssanthacopoulos, J., Deryng, D., Elliott, J., Folberth, C., Khabarov, N., Muller, C., Olin, S., Pugh, T.A.M., Schaphoff, S., Schewe, J., Schmid, E., Warszawski, L., Levermann, A., 2017. Understanding the weather signal in national crop-yield variability. *Earths Future* 5, 605–616. <https://doi.org/10.1002/2016ef000525>.
- Godfray, H.C.J., Beddington, J.R., Crute, I.R., Haddad, L., Lawrence, D., Muir, J.F., Pretty, J., Robinson, S., Thomas, S.M., Toulmin, C., 2010. Food Security: The Challenge of Feeding 9 Billion People. 327, 812–818. <https://doi.org/10.1126/science.118538>.
- Grosz, B., Dechow, R., Gebbert, S., Hoffmann, H., Zhao, G., Constantin, J., Raynal, H., Wallach, D., Coucheney, E., Lewan, E., Eckersten, H., Specka, X., Kersebaum, K.C., Nendel, C., Kuhnert, M., Yeluripati, J., Haas, E., Teixeira, E., Bindi, M., Trombi, G., Moriondo, M., Doro, L., Roggero, P.P., Zhao, Z.G., Wang, E.L., Tao, F.L., Rotter, R., Kassie, B., Cammarano, D., Asseng, S., Weihermüller, L., Siebert, S., Gaiser, T., Ewert, F., 2017. The implication of input data aggregation on up-scaling soil organic carbon changes. *Environ. Model. Softw.* 96, 361–377. <https://doi.org/10.1016/j.envsoft.2017.06.046>.
- Gustafsson, D., Lewan, E., Jansson, P.-E., 2004. Modeling water and heat balance of the boreal landscape—comparison of Forest and arable land in Scandinavia. *J. Appl. Meteorol.* 43, 1750–1767. <https://doi.org/10.1175/JAM2163.1>.
- Hansen, J.W., Jones, J.W., 2000. Scaling-up crop models for climate variability applications. *Agric. Syst.* 65, 43–72. [https://doi.org/10.1016/S0308-521X\(00\)00025-1](https://doi.org/10.1016/S0308-521X(00)00025-1).
- He, W., Yang, J.Y., Qian, B., Drury, C.F., Hoogenboom, G., He, P., Lapen, D., Zhou, W., 2018. Climate change impacts on crop yield, soil water balance and nitrate leaching in the semiarid and humid regions of Canada. *PLoS One* 13. <https://doi.org/10.1371/journal.pone.0207370>.
- He, Y., Shi, Y.L., Liang, H., Hu, K.L., Hou, L.L., 2020. Soil water and nitrogen fluxes in response to climate change in a wheat-maize double cropping system. *Agronomy* 10, 13. <https://doi.org/10.3390/agronomy10060786>.
- Hoffmann, H., Zhao, G., van Bussel, L.G.J., Enders, A., Specka, X., Sosa, C., Yeluripati, J., Tao, F., Constantin, J., Raynal, H., Teixeira, E., Grosz, B., Doro, L., Zhao, Z., Wang, E., Nendel, C., Kersebaum, K.C., Haas, E., Kiese, R., Klatt, S., Eckersten, H., Vanuytrecht, E., Kuhnert, M., Lewan, E., Rotter, R., Roggero, P.P., Wallach, D., Cammarano, D., Asseng, S., Krauss, G., Siebert, S., Gaiser, T., Ewert, F., 2015. Variability of effects of spatial climate data aggregation on regional yield simulation by crop models. *Clim. Res.* 65, 53–69. <https://doi.org/10.3354/cr01326>.
- Hoffmann, H., Zhao, G., Asseng, S., Bindi, M., Biernath, C., Constantin, J., Coucheney, E., Dechow, R., Doro, L., Eckersten, H., Gaiser, T., Grosz, B., Heinlein, F., Kassie, B.T., Kersebaum, K.C., Klein, C., Kuhnert, M., Lewan, E., Moriondo, M., Nendel, C., Priesack, E., Raynal, H., Roggero, P.P., Rotter, R.P., Siebert, S., Specka, X., Tao, F.L., Teixeira, E., Trombi, G., Wallach, D., Weihermüller, L., Yeluripati, J., Ewert, F., 2016b. Impact of Spatial Soil and Climate Input Data Aggregation on Regional Yield Simulations. *PLoS One* 11, 23. <https://doi.org/10.1371/journal.pone.0151782>.
- Hoffmann, H., Enders, A., Siebert, S., Gaiser, T., Ewert, F., 2016a. Climate and soil input data aggregation effects in crop models. *Harvard Dataverse*. <https://doi.org/10.7910/DVN/COJ5BB>.
- Hristov, J., Toreti, A., Pérez Domínguez, I., Dentener, F., Fellmann, T., Elleby, C., Ceglár, A., Fumagalli, D., Niemeyer, S., Cerrani, I., Panarello, L., Bratu, M., 2020. Analysis of Climate Change Impacts on EU Agriculture by 2050, EUR 30078EN. Publications Office of the European Union, Luxembourg.
- Jansson, P.E., 2012. CoupModel: model use, calibration and validation. *Trans. ASABE* 55, 1337–1346. <https://doi.org/10.13031/2013.42245>.
- Jansson, P.E., Karlberg, L., 2013. Coupled Heat and Mass Transfer Model for Soilplant -Atmosphere System. (WWW Document).
- Jones, L., Provens, A., Holland, M., Mills, G., Hayes, F., Emmett, B., Hall, J., Sheppard, L., Smith, R., Sutton, M., Hicks, K., Ashmore, M., Haines-Young, R., Harper-Simmonds, L., 2014. A review and application of the evidence for nitrogen impacts on ecosystem services. *Ecosyst. Serv.* 7, 76–88. <https://doi.org/10.1016/j.ecoser.2013.09.001>.
- Kaye, J.P., Quemada, M., 2017. Using cover crops to mitigate and adapt to climate change. A review. *Agron. Sustain. Dev.* 37. <https://doi.org/10.1007/s13593-016-0410-x>.
- Kuhnert, M., Yeluripati, J., Smith, P., Hoffmann, H., van Oijen, M., Constantin, J., Coucheney, E., Dechow, R., Eckersten, H., Gaiser, T., Grosz, B., Haas, E., Kersebaum, K.C., Kiese, R., Klatt, S., Lewan, E., Nendel, C., Raynal, H., Sosa, C., Specka, X., Teixeira, E., Wang, E.L., Weihermüller, L., Zhao, G., Zhao, Z.G., Ogle, S., Ewert, F., 2017. Impact analysis of climate data aggregation at different spatial scales on simulated net primary productivity for croplands. *Eur. J. Agron.* 88, 41–52. <https://doi.org/10.1016/j.eja.2016.06.005>.
- Leng, G., Hall, J., 2019. Crop yield sensitivity of global major agricultural countries to droughts and the projected changes in the future. *Sci. Total Environ.* 654, 811–821. <https://doi.org/10.1016/j.scitotenv.2018.10.434>.
- Loecke, T.D., Burgin, A.J., Riveros-Iregui, D.A., Ward, A.S., Thomas, S.A., Davis, C.A., Clair, M.A.S., 2017. Weather whiplash in agricultural regions drives deterioration of water quality. *Biogeochemistry* 133, 7–15. <https://doi.org/10.1007/s10533-017-0315-z>.
- Ludwig, F., Asseng, S., 2006. Climate change impacts on wheat production in a Mediterranean environment in Western Australia. *Agric. Syst.* 90, 159–179. <https://doi.org/10.1016/j.agsy.2005.12.002>.
- Maharjan, G.R., Hoffmann, H., Webber, H., Srivastava, A.K., Weihermüller, L., Villa, A., Coucheney, E., Lewan, E., Trombi, G., Moriondo, M., Bindi, M., Grosz, B., Dechow, R., Kuhnert, M., Doro, L., Kersebaum, K.-C., Stella, T., Specka, X.,

- Nendel, C., Constantin, J., Raynal, H., Ewert, F., Gaiser, T., 2019. Effects of input data aggregation on simulated crop yields in temperate and Mediterranean climates. *Eur. J. Agron.* 103, 32–46. <https://doi.org/10.1016/j.eja.2018.11.001>.
- Martre, P., Wallach, D., Asseng, S., Ewert, F., Jones, J.W., Rotter, R.P., Boote, K.J., Ruane, A.C., Thorburn, P.J., Cammarano, D., Hatfield, J.L., Rosenzweig, C., Aggarwal, P.K., Angulo, C., Basso, B., Bertuzzi, P., Biernath, C., Brisson, N., Challinor, A.J., Doltra, J., Gayler, S., Goldberg, R., Grant, R.F., Heng, L., Hooker, J., Hunt, L.A., Ingwersen, J., Izaurralde, R.C., Kersebaum, K.C., Muller, C., Kumar, S.N., Nendel, C., O'Leary, G., Olesen, J.E., Osborne, T.M., Palosuo, T., Priesack, E., Ripoche, D., Semenov, M.A., Shcherbak, I., Steduto, P., Stockle, C.O., Stratonovitch, P., Streck, T., Supit, I., Tao, F.L., Travasso, M., Waha, K., White, J.W., Wolf, J., 2015. Multimodel ensembles of wheat growth: many models are better than one. *Glob. Change Biol.* 21, 911–925. <https://doi.org/10.1111/gcb.12768>.
- Matiu, M., Ankerst, D.P., Menzel, A., 2017. Interactions between temperature and drought in global and regional crop yield variability during 1961–2014. *PLoS One* 12, e0178339. <https://doi.org/10.1371/journal.pone.0178339>.
- Morrison, B.D., Heath, K., Greenberg, J.A., 2019. Spatial scale affects novel and disappeared climate change projections in Alaska. *Ecol. Evol.* 9, 12026–12044. <https://doi.org/10.1002/ece3.5511>.
- Neil Adger, W., Arnell, N.W., Tompkins, E.L., 2005. Successful adaptation to climate change across scales. *Glob. Environ. Change* 15, 77–86. <https://doi.org/10.1016/j.gloenvcha.2004.12.005>.
- Nouri, M., Homae, M., Bannayan, M., Hoogenboom, G., 2016. Towards modeling soil texture-specific sensitivity of wheat yield and water balance to climatic changes. *Agric. Water Manag.* 177, 248–263. <https://doi.org/10.1016/j.agwat.2016.07.025>.
- Olesen, J.E., Bindi, M., 2002. Consequences of climate change for European agricultural productivity, land use and policy. *Eur. J. Agron.* 16, 239–262. [https://doi.org/10.1016/s1161-0301\(02\)00004-7](https://doi.org/10.1016/s1161-0301(02)00004-7).
- Olesen, J.E., Trnka, M., Kersebaum, K.C., Skjelvag, A.O., Seguin, B., Pelttonen-Sainio, P., Rossi, F., Kozyra, J., Micale, F., 2011. Impacts and adaptation of European crop production systems to climate change. *Eur. J. Agron.* 34, 96–112. <https://doi.org/10.1016/j.eja.2010.11.003>.
- Olesen, J.E., Borgeas, C.D., Elsgaard, L., Palosuo, T., Rotter, R.P., Skjelvag, A.O., Pelttonen-Sainio, P., Borjesson, T., Trnka, M., Ewert, F., Siebert, S., Brisson, N., Eitzinger, J., van Asselt, E.D., Oberforster, M., van der Fels-Klerx, H.J., 2012. Changes in time of sowing, flowering and maturity of cereals in Europe under climate change. *Food Addit. Contam. Part A-Chem.* 29, 1527–1542. <https://doi.org/10.1080/19440049.2012.712060>.
- Rezaei, E.E., Siebert, S., Hüging, H., Ewert, F., 2018. Climate change effect on wheat phenology depends on cultivar change. *Sci. Rep.* 8, 4891. <https://doi.org/10.1038/s41598-018-23101-2>.
- Ribeiro, A.F.S., Russo, A., Gouveia, C.M., Pascoa, P., 2019. Modelling drought-related yield losses in Iberia using remote sensing and multiscalar indices. *Theor. Appl. Climatol.* 136, 203–220. <https://doi.org/10.1007/s00704-018-2478-5>.
- Rosenzweig, C., Elliott, J., Deryng, D., Ruane, A.C., Muller, C., Arneth, A., Boote, K.J., Folberth, C., Glotter, M., Khabarov, N., Neumann, K., Piontek, F., Pugh, T.A.M., Schmid, E., Stehfest, E., Yang, H., Jones, J.W., 2014. Assessing agricultural risks of climate change in the 21st century in a global gridded crop model intercomparison. *Proc. Natl. Acad. Sci. U.S.A.* 111, 3268–3273. <https://doi.org/10.1073/pnas.1222463110>.
- Ruane, A.C., Goldberg, R., Chryssanthacopoulos, J., 2015. Climate forcing datasets for agricultural modeling: merged products for gap-filling and historical climate series estimation. *Agric. Meteorol.* 200, 233–248. <https://doi.org/10.1016/j.agrformet.2014.09.016>.
- Semenov, M.A., 2009. Impacts of climate change on wheat in England and Wales. *J. R. Soc. Interface* 6, 343–350. <https://doi.org/10.1098/rsif.2008.0285>.
- SOU, 2007. Sverige inför klimatförändringarna – hot och möjligheter. Slutbetänkande av klimat- och sårbarhetsutredningen. Statens offentliga utredningar, S. Stockholm, p. 188. (<https://www.regeringen.se/49bbac/contentassets/94b5ab7c66604cd0b8842fd6510b42c9/sverige-infor-klimatforandringarna-hot-och-mojligheter-missiv-ka-pitel-1-3-sou-200760>).
- Stuart, M.E., Goody, D.C., Bloomfield, J.P., Williams, A.T., 2011. A review of the impact of climate change on future nitrate concentrations in groundwater of the UK. *Sci. Total Environ.* 409, 2859–2873. <https://doi.org/10.1016/j.scitotenv.2011.04.016>.
- Thorntwaite, C.W., 1948. An approach toward a rational classification of climate. *Geogr. Rev.* 38, 55–94. <https://doi.org/10.2307/210739>.
- Tijdeman, E., Menzel, L., 2020. Controls on the development and persistence of soil moisture drought across Southwestern Germany. *Hydrol. Earth Syst. Sci. Discuss.* 2020, 1–20. <https://doi.org/10.5194/hess-2020-307>.
- de Toro, A., Eckersten, H., Nkurunziza, L., von Rosen, D., 2015. Effects of extreme weather on yield of major arable crops in Sweden. *Swed. Univ. Agric. Sci.* 308. (https://pub.epsilon.slu.se/12606/8/deToro_a_et_al_151109.pdf).
- Trnka, M., Feng, S., Semenov, M.A., Olesen, J.E., Kersebaum, K.C., Rötter, R.P., Semerádová, D., Klem, K., Huang, W., Ruiz-Ramos, M., Hlavinka, P., Meitner, J., Balek, J., Havlík, P., Büntgen, U., 2019. Mitigation efforts will not fully alleviate the increase in water scarcity occurrence probability in wheat-producing areas. *Sci. Adv.* 5, eaau2406. <https://doi.org/10.1126/sciadv.aau2406>.
- van Etten, J., de Sousa, K., Aguilar, A., Barrios, M., Coto, A., Dell'Acqua, M., Fadda, C., Gebrehawaryat, Y., van de Gevel, J., Gupta, A., Kiros, A.Y., Madriz, B., Mathur, P., Mengistu, D.K., Mercado, L., Mohammed, J.N., Paliwal, A., Pe, M.E., Quiros, C.F., Rosas, J.C., Sharma, N., Singh, S.S., Solanki, I.S., Steinke, J., 2019. Crop variety management for climate adaptation supported by citizen science. *Proc. Natl. Acad. Sci. U.S.A.* 116, 4194–4199. <https://doi.org/10.1073/pnas.1813720116>.
- Vicente-Serrano, S.M., Begueria, S., Lopez-Moreno, J.I., 2010. A multiscalar drought index sensitive to global warming: the standardized precipitation evapotranspiration index. *J. Clim.* 23, 1696–1718. <https://doi.org/10.1175/2009jcli2909.1>.
- Wang, B., Feng, P., Liu, D.L., O'Leary, G.J., Macadam, I., Waters, C., Asseng, S., Cowie, A., Jiang, T., Xiao, D., Ruan, H., He, J., Yu, Q., 2020. Sources of uncertainty for wheat yield projections under future climate are site-specific. *Nat. Food.* <https://doi.org/10.1038/s43016-020-00181-w>.
- Wang, J., Wang, E.L., Yang, X.G., Zhang, F.S., Yin, H., 2012. Increased yield potential of wheat-maize cropping system in the North China Plain by climate change adaptation. *Clim. Change* 113, 825–840. <https://doi.org/10.1007/s10584-011-0385-1>.
- Webber, H., Zhao, G., Wolf, J., Britz, W., de Vries, W., Gaiser, T., Hoffmann, H., Ewert, F., 2015. Climate change impacts on European crop yields: Do we need to consider nitrogen limitation? *Eur. J. Agron.* 71, 123–134. <https://doi.org/10.1016/j.eja.2015.09.002>.
- Webber, H., Ewert, F., Olesen, J.E., Müller, C., Fronzek, S., Ruane, A.C., Bourgault, M., Martre, P., Ababaei, B., Bindi, M., Ferrise, R., Finger, R., Fodor, N., Gabaldón-Leal, C., Gaiser, T., Jabloun, M., Kersebaum, K.-C., Lizaso, J.I., Lorite, I.J., Manceau, L., Moriando, M., Nendel, C., Rodríguez, A., Ruiz-Ramos, M., Semenov, M. A., Siebert, S., Stella, T., Stratonovitch, P., Trombi, G., Wallach, D., 2018. Diverging importance of drought stress for maize and winter wheat in Europe. *Nat. Commun.* 9, 4249. <https://doi.org/10.1038/s41467-018-06525-2>.
- Webber, H., Lischeid, G., Sommer, M., Finger, R., Nendel, C., Gaiser, T., Ewert, F., 2020. No perfect storm for crop yield failure in Germany. *Environ. Res. Lett.* 15, 104012.
- Zhao, G., Siebert, S., Enders, A., Rezaei, E.E., Yan, C.Q., Ewert, F., 2015. Demand for multi-scale weather data for regional crop modeling. *Agric. Meteorol.* 200, 156–171. <https://doi.org/10.1016/j.agrformet.2014.09.026>.
- Zscheischler, J., Westra, S., van den Hurk, B.J.J.M., Seneviratne, S.I., Ward, P.J., Pitman, A., Aghakouchak, A., Bresch, D.N., Leonard, M., Wahl, T., Zhang, X., 2018. Future climate risk from compound events. *Nat. Clim. Change* 8, 469–477. <https://doi.org/10.1038/s41558-018-0156-3>.